Production of Magnetic Nanoparticles in Imine Polymer Matrixes

Cristina Castro,[†] José Ramos,[†] Angel Millán,*[,†] José González-Calbet,[‡] and Fernando Palacio[†]

Instituto de Ciencia de Materiales de Aragón, CSIC−Universidad de Zaragoza, 50009 Zaragoza, Spain, and Depto. de Química Inorgánica, Universidad Complutense, 28040 Madrid, Spain

Received August 4, 2000. Revised Manuscript Received September 21, 2000

Nanocomposites showing superparamagnetic properties have been synthesized from imine polymers. The method for the production of the nanocomposites is very simple. The imine polymer reacts with a metal salt and the product is dried. Apparently, the reaction of polymer grains with a metal solution takes place by a surface reaction mechanism. Metal hydroxides precipitate within the polymer matrix without addition of a base or of an oxidizer since the polymer imine groups provide a basic medium. The metal oxides are formed through hydrolysis of the metal hydroxides when drying. The method works the best for imine polymers with a flexible chain and no hydrophobic branches. Several iron and cobalt salts, as well as a manganese salt, have been used in the procedure. The effect of the solvent and of the metal salt counterion on the procedure has been studied.

Introduction

Nanoparticles can be produced by a wide variety of methods. They have been obtained from solid phase,[1] gas phase,[2] melt,[3] or solution.[4−6] The problems in the production of nanoscale particles arise from their facility to aggregate and the difficulties in controlling their size. These problems can be avoided in several ways: (1) by covering the nanoparticles with a protective layer;[7] (2) by fixing the particles to a substrate (fiber,[8] monolayer,[9] multilayer,[10] film,[11] or block[12]); (3) by precipitating the particles in a confined space (reverse micelles,[13] activated surface,[14] film,[15] gel,[16] zeolite,[17] glass,[18] organic polymer,[19−25] other solid matrix,[26] or even a liquid crystal[27]). The choice for the most suitable method will depend on the application wanted for the material. A good way to control the size and size distribution of growing particles is to make use of organic polymers. In addition, this method yields composites with a low specific weight, high homogeneity, and high processability.

There are several approaches for the production of polymer nanocomposites. The ex situ approach consists of the precipitation of nanoparticles by a sol−gel, reverse micelles, or other method, followed by consolidation of the material. In the in situ approach, the nanoparticles are grown within a polymer matrix. The particles are usually precipitated from a metal salt embedded in the polymer. An alternative procedure is the decomposition

[†] CSIC−Universidad de Zaragoza.
[‡] Universidad Complutense.

(1) Ko, M. J.; Birnboim, M.; Plawsky, J. *Adv. Mater.* **1997**, *9*, 909.
(2) Suenaga, K.; Colliex, C.; Demoncy, N.; Loiseau, A.; Pascard, H.; Willaime, F. *Science* **1997**, *278*, 653.
(3) Champion, Y.; Bigot, *J. Mater Sci. Eng. A−Struct. Mater.* **1996**, *217*, 58.
(4) Kang, Y. S.; Risbud, S.; Rabolt, J. F.; Stroeve, P. *Chem. Mater.* **1996**, *8*, 2209.
(5) Trindade, T.; Obrien, P. *J. Mater. Chem.* **1996**, *6*, 343.
(6) Ponomarev, E. A.; Albuyaron, A.; Tenne, R.; Levyclement, C. *J. Electrochem. Soc.* **1997**, *144*, L277.
(7) Bidan, G.; Jarjayes, O.; Fruchart, J. M.; Hannecart, E. *Adv. Mater.* **1994**, *6*, 152.
(8) Lizmarzan, L. M.; Philipse, A. P. *J. Phys. Chem.* **1995**, *99*, 15120.
(9) Fendler, J. H.; Meldrum, F. C. *Adv. Mater.* **1995**, *7*, 607.
(10) Schmitt, J.; Decher, G.; Dressick, W. J.; Brandow, S. L.; Geer, R. E.; Shashidhar, R.; Calvert, J. M. *Adv. Mater.* **1997**, *9*, 61.
(11) Zhang, P.; Yang, Z. H.; Wang, D. J.; Kan, S. H.; Chai, X. D.; Liu, J. Z.; Li, T. J. *Synth. Met.* **1997**, *84*, 165.
(12) John, V. T.; Mcpherson, G. L.; Akkara, J. A.; Kaplan, D. L. *J. Appl. Phys.* **1997**, *81*, 4741.
(13) Kommaredi, N. S.; Tata, M.; John, V. T.; Pherson, G. L.; Herman, M. F. *Chem. Mater.* **1996**, *8*, 801.
(14) Palacin, S.; Hidber, P. C.; Bourgoin, J. P.; Miramond, C.; Fermon, C.; Whitesides, G. M. *Chem. Mater.* **1996**, *8*, 1316.
(15) Bunker, B. C.; Rieke, P. C.; Tarasevich, B. J.; Campbell, A. A.; Fryxell, G. E.; Graff, G. L.; Song, L.; Liu, J.; Virden, J. W.; McVay, G. L. *Science* **1994**, *264*, 48.
(16) Schubert, U.; Tewinkel, S.; Lamber, R. *Chem. Mater.* **1996**, *8*, 2047.
(17) García, J. L.; López, A.; Lázaro, F. J.; Martínez, C.; Corma, A. *J. Magn. Magn. Mater.* **1996**, *157*, 272.
(18) Tsang, C.; Gafney, H. D.; Sunil, D.; Rafailovich, M.; Sokolov, J.; Gambino, R. J. *J. Appl. Phys.* **1996**, *79*, 6025.
(19) Ziolo, R. F.; Giannelis, E. P.; Weinstein, B. A.; O'Horo, M. P.; Ganguli, B. N.; Mehrotra, V.; Russell, M. W.; Huffman, D. R. *Science* **1992**, *257*, 219.
(20) Nguyen, M. T.; Díaz, A. F. *Adv. Mater.* **1994**, *6*, 858.
(21) Raymond, L.; Revol, J.-F.; Ryan, D. H.; Marchessault, R. H. *Chem. Mater.* **1994**, *6*, 249.
(22) Sohn, B. H.; Cohen, R. E. *Chem. Mater.* **1997**, *9*, 264.
(23) Cheong Chan, Y. Ng.; Craig, G. S. W.; Schrock, R. R.; Cohen, R. E. *Chem. Mater.* **1992**, *4*, 885.
(24) Wosniak, M. E.; Sen, A.; Rheingold, A. L. *Chem. Mater.* **1992**, *4*, 753.
(25) Cho, C. S.; Jeong, Y. I.; Ishihara, T.; Takei, R.; Park, J. U.; Park, K. H.; Maruyama, A.; Akaike, T. *Bio. Mater.* **1997**, *18*, 323.
(26) Yang, W.; Inoue, H.; Nakazono, Y.; Samura, H.; Saegusa, T. *ACS Symp. Ser.* **1996**, *622*, 205. (b) Rhie, K.; Naugle, D. G.; O, B. H.; Markert, J. T.; Morrish, A. H.; Zhou, X. Z. *J. Phys.-Condensed Mater.* **1996**, *7*, 3315. (c) Abe, T.; Tachibana, Y.; Uematsu, T.; Iwamoto, M. *J. Chem. Soc.-Chem. Commun.* **1995**, *16*, 1617. (d) Ayyappan, S.; Rao, C. N. R. *Eur. J. Solid State Inorg. Chem.* **1996**, *33*, 737. (e) Sloan, J.; Cook, J.; Green, M. L. H.; Hutchison, J. L.; Tenne, R. J. *Mater. Chem.* **1997**, *7*, 1089.
(27) Chen, J. P.; Nikles, D. E. *IEEE Trans. Magn.* **1996**, *32*, 4478.

10.1021/cm0011561 CCC: $19.00
Published on Web 11/16/2000

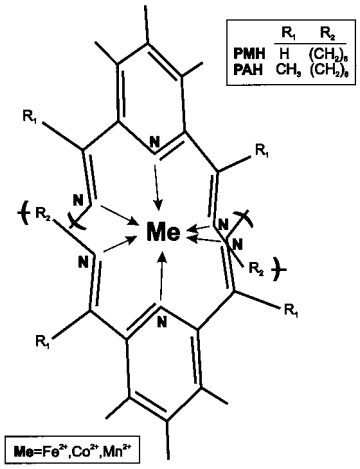

Figure 1. Structure of the imine−metal complex found by EXAFS.

of a metal−organic precursor by thermal treatment.[28] Several organic polymers have been used for the production of magnetic nanocomposites. Early materials were inspired by biological mineralization processes and consisted of long aliphatic chains with amino acid and amine moieties.[29] Thereafter, a large variety of polymers have been used, including maleic anhydride polymers,[4] phenolic polymers,[13] polypyrrole,[7] polysaccharides,[30] sulfonated polystyrene resins,[19] sulfonated polypyrrole linear polymers,[20] sulfonated cellulosics,[21] etc. A sophisticated approach to optimize the control of the size, size dispersion, shape, and distribution in the matrix of the particles is based on the use of block copolymers with hydrophilic and hydrophobic parts that provide a uniform distribution of polar nanodomains for the precipitation of the inorganic particles.[22]

Most of polymers used in the preparation of magnetic nanocomposites contain charged groups for the interaction with precursor metal salts. However, neutral polymers may be advantageous concerning processability and versatility. This paper is dealing with the production of metal oxide magnetic nanoparticles inside a neutral polymer matrix such as polyimines. These polymers form stable complexes with divalent transition metal ions.[31] Early studies of polyimine−iron materials interpreted their unusual magnetic properties as intrinsic to the polymer−metal complex.[32] Later, it was demonstrated that superparamagnetic behavior in these materials was related to the presence of iron oxide nanoparticles formed during the preparation of the polymer complex.[33] Magnetic measurements of polyimine−cobalt(II) complexes also revealed a superparamagnetic behavior.[34] According to EXAFS and XANES studies[35] the structure of the Fe(II) and Co(II) polymer complexes is that shown in Figure 1.

The aim of this work is to present a very simple way to obtain magnetic nanocomposites from polyimine polymers. The advantage of these polymers is that they produce magnetic nanoparticles directly by suspension in a metal salt without any basic or oxidizing treatment. Materials have been prepared from two different polyimines and several precursor metal salts. The reaction of the polymer with the metal solution has been investigated by optical microscopy, X-ray diffraction, differential thermal analysis, and IR and NMR spectroscopy. The materials have been characterized by electron microscopy, and their magnetic properties have been measured. The mechanism of the reaction has been studied and the effect of the polymer structure, the solvent, and the anion precursor salt on the properties of the nanocomposite is discussed.

Experimental Section

Chemicals and Reagents. High purity reagents were purchased from Aldrich or Fluka. Solvents were dried following the standard procedure and deoxygenated under an argon flow.

Monomers. 2,6-Pyridinedicarboxaldehyde was synthesized by adding 3.98 g of SeO_2 to 60 mL of a dioxane solution containing 5 g of 2,6-bis(hydroximethyl)pyridine and stirring under reflux during 4 h. After vacuum evaporation of the solvent, the precipitate was purified by continuous extraction in a Soxhlet with petroleum ether and further sublimation at 0.1 torr and 80 °C. The reaction yielded 3.5 g of white crystalline solid.

Polymers. Poly[2,6-pyridinebis(methylidene)hexamethylenediamine] (PMH) was prepared following the method described by Lions and Martin[31] by mixing ethanol solutions of the 2,6-pyridinedicarboxaldehyde and 1,6-hexanediamine under reflux in an inert atmosphere. The resulting precipitate was filtered and washed with ethanol and ether. The product was characterized by elemental analysis, IR, NMR, viscosity measurements, and DSC. The polymer poly[2,6-pyridine-bis-((α-methyl)methylidene)hexamethylenediamine] (PAH) was synthesized in a similar way.

Polymer Complexes. Several polymer−coordination compounds were prepared by suspending the polymers in a solution of the metal salts. The metal salts used in the experiments were $FeSO_4 \cdot 7H_2O$, $FeCl_2 \cdot 6H_2O$, $CoSO_4 \cdot 7H_2O$, $Co(NO_3)_2 \cdot 6H_2O$, $Co(ClO_4)_2 \cdot 6H_2O$, $CoCl_2 \cdot 6H_2O$, $CoCl_2$, and $Mn(ClO_4)_2 \cdot 6H_2O$.

A typical procedure for the preparation of the polymer−metal complex was the following: a solution of $FeSO_4 \cdot 7H_2O$ in boiling water (3.72 mM, 10 mL) was added through Kieselghur, to eliminate any trace of iron hydroxide colloid, to a suspension of the PMH polymer in water (1.86 mM, 5 mL). The white polymer powder turned violet immediately after addition. The suspension was kept 1 h under stirring at 80 °C. The resulting solid was filtered and washed with deoxygenated water. Then, it was dried under vacuum at ambient temperature in the presence of KOH and P_2O_5.

Several material samples were prepared with methanol, ethanol, ethylene glycol, a glycerin−water mixture, and an acetone−water mixture as a solvent. Other samples were prepared under anhydrous conditions throughout the procedure. Some PMH−Co samples were prepared by a homogeneous method that consisted of mixing a solution of the polymer in chloroform with a solution of the metal salt in water.

The in situ optical microscopy observations of the reaction process were carried out by placing drops of a polymer suspension between two microscope slide covers and feeding the system laterally with the metal solution.

Measurements. All compounds prepared in this work were characterized and identified by elemental analysis, FTIR,

(28) Borelli, N. F.; Morse, D. L.; Schreurs, J. W. H. *J. Appl. Phys.* **1983**, *54*, 3344.
(29) Okada, H.; Sakata, K.; Kunitake, T. *Chem. Mater.* **1990**, *2*, 89.
(30) Kroll, E.; Winnik, F. M. *Chem. Mater.* **1996**, *8*, 1594.
(31) Lions, F.; Martin, K. V. *J. Am. Chem. Soc.* **1957**, *79*, 2733.
(32) Sugano, T.; Nomura, M.; Awaga, K.; Poh, L. K.; Ohta, T.; Kinoshita, M. *Bull. Chem. Soc. Jpn.* **1986**, *59*, 2615.
(33) Palacio, F.; Castro, C.; Reyes, J.; Sturgeon, G.; Lázaro, F. J. In *Physics and Chemistry of Finite Systems: From Clusters to Crystals*; Jena, P., Ed.; Kluwer Academic Publishers: Amsterdam, 1992; Vol. I, p 793.
(34) Palacio, F.; Castro, C.; Lázaro, F. J.; Reyes, J. *J. Magn. Magn. Mater.* **1992**, *104*, 2101.
(35) García, J.; Chaboy, J.; Marguin, V.; Castro, C.; Ramos, J.; Palacio, F. *Jpn. J. Appl. Phys.* **1993**, *32*, 800.

Table 1. Characteristics of the Polymers

	PMH	PMH−$FeSO_4$	PMH−$CoSO_4$	PAH	PAH−$FeCl_2$	PAH−$CoCl_2$
color	white	violet	brown	white	dark violet	brown
ν(C═N)	1646	1526	1653	1630	1598	1584
mp °C	130−150	300 (dec.)	280 (dec.)	100−140	>300	173

NMR, and mass spectroscopy when possible. Elemental analysis of carbon, hydrogen, and nitrogen was performed in a Perkin-Elmer 248B analyzer. Metal contents were determined by atomic absorption spectrometry in a plasma analyzer, Perkin-Elmer Plasma 40. FTIR spectra in a range 400−4000 cm^{-1} were recorded on a Perkin-Elmer 1600 using the conventional KBr pellet technique. NMR spectra were recorded either on a Varian XL200 MHz or on a Variant Unity 300 MHz instrument, from solutions of the materials in $CDCl_3$. Thermogravimetry (TGA) and differential scanning calorimetry (DSC) were performed on Perkin-Elmer TGS2 and DSC-7 instruments, under N_2 flow, at a heating rate of 10 °C/min. X-ray powder diffraction data were collected on a Siemens D501 diffractometer with Cu Kα radiation, in the range $5° < 2\theta < 100°$, with step size 0.04°. Magnetic measurements of material powders enclosed in 5 × 15 mm gelatin capsules were carried out on a home designed ac susceptometer[37] and in a SQUID magnetometer from Quantum Design, model MPMS, in the temperature range 1.8−300 K.

TEM observations were carried out on a JEOL 2000FX/II microscope equipped with a Link Analytical eXL system for EDS analysis. Samples were prepared by dividing the beads in an agate mortar to an appropriate size, dispersing the grains in *n*-butanol, and extending the suspension on a copper grid coated with carbon. Other samples were embedded in an epoxy block, cut into ultrathin sections, and deposited on a copper grid.

Results

PMH Polymer. Samples of PMH prepared by the method described in the Experimental Section were analyzed by NMR spectroscopy. A polymer chain length of 50 units was estimated from the area ratio of the terminal aldehyde proton and the aromatic proton peaks. This value is consistent with molecular weight calculations and viscosimetry measurements. The melting temperature of PMH measured by DSC was 130−150 °C (Table 1). Such a narrow range indicates a uniform chain length.

Reaction of PMH with a Metal Salt. PMH powders react with Fe(II), Co(II), and Mn(II) solutions with a change of color. Figure 2 shows the IR spectra of PMH before and after reaction with $FeSO_4$. The spectrum of PMH shows a band at 1646 cm^{-1} that is characteristic of imine bond stretching vibration. This band shifts after reaction, suggesting the formation of coordination bonds between the imine π orbital and the metal ions. The polymer−metal complex materials resulting from the reaction of PMH with iron and cobalt salts decompose before melting at temperatures near 300 °C (Table 1). Thus, the thermal stability of the polymer−metal complex material is much higher than that of the pure polymer. Analyses of materials by powder X-ray diffraction show an increase of the structural disorder in the polymer−metal complex material with respect to the pure polymer.

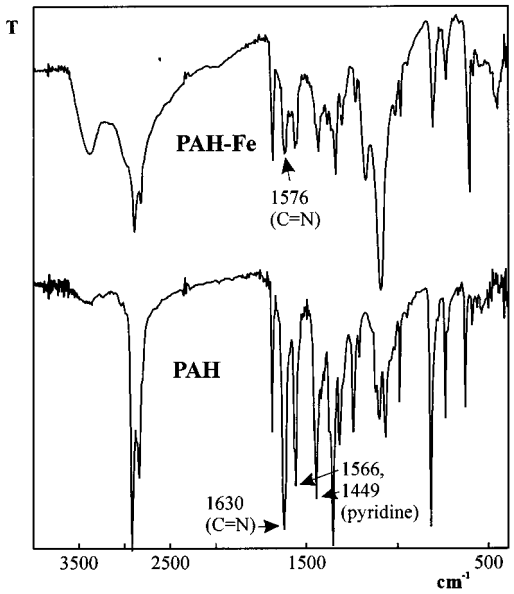

Figure 2. FTIR spectra of PMH and a PMH−Fe material sample obtained from $FeSO_4$.

The progress of the reaction was established by making consecutive X-ray diffraction patterns and IR spectra. The evolution of the polymer grains during reaction with the metal solution was observed by optical microscopy. The reaction does not begin along the whole grain surface. It starts on surface irregularities and then extends across the surface and inward the grain. At an intermediate stage, the reacted material separates easily from the rest of the grain. The texture of the final material after reaction and before drying is that of a transparent uniform gel.

Characteristics of PMH−Metal Complex Materials. *Composition*. The characteristics of the resulting PMH−metal complex materials are shown in Table 2. Despite a high excess of metal ions used in the reaction of the polymer with the metal solution, the monomer/metal ratio was found to be close to 2, when the solvent was water. This ratio corresponds to the structure of the polyimine−iron(II) complex found by EXAFS.[35] When the reaction was carried out in ethanol or chloroform solutions the monomer/metal ratio was close to 1.

Influence of the Metal Ion. Figure 3A shows TEM images of a composite sample prepared from $FeSO_4$ and PMH. Two different crystal populations can be distinguished in this sample. The first one consists of linear crystal aggregates with a thickness of 10−15 nm and a length of 70−150 nm. The second one consists of polyhedral crystals with a size of 10−30 nm. Electron diffraction patterns on an area comprising several nanocrystals correspond to a superposition of goethite (α-FeOOH) and hematite (α-Fe_2O_3) crystal structures. Some large particles were analyzed individually and their patterns corresponded to hematite (upper left side in Figure 3A). Figure 3B shows a TEM image of a PMH−Fe composite sample prepared from an iron(II)

(36) Castro, C.; et al. In preparation.

(37) Rillo, C.; Lera, F.; Badía, A.; Angurel, L. A.; Bartolomé, J.; Palacio, F.; Navarro R.; van Duyneveldt, A. J. In *Magnetic Susceptibility of Superconductors and other Spin Systems*; Hein, R. A., Francavilla, T. L., Liedenberg, D. H., Eds.; Plenum Press: New York, 1991; pp 1−24.

Table 2. Characteristics of the PMH composites

	salt										
	$FeSO_4 \cdot 7H_2O$	$FeSO_4 \cdot 7H_2O$	$FeSO_4 \cdot 7H_2O$	$FeCl_2 \cdot 4H_2O$	$CoSO_4 \cdot 7H_2O$	$CoSO_4 \cdot 7H_2O$	$CoCl_2 \cdot 6H_2O$	$CoCl_2 \cdot 6H_2O$	$Co(NO_3)_2 \cdot 6H_2O$	$Co(ClO_4)_2 \cdot 6H_2O$	$Mn(ClO_4)_2 \cdot 6H_2O$
solvent	water	water	water	water	water	chloroform/ water	water	ethanol	water	water	water
method	standard	additive $Na_2S_2O_3$	additive EDTA	standard	standard	polymer solution	standard	standard	standard	standard	standard
[monomer]/[metal]	2	1.7	1.7	2		1	2	1	1.7	2	1.9
particles	yes	yes	yes	yes	yes	non	yes	yes	yes	yes	non
structure	α-Fe_2O_3, α-FeOOH	α-FeOOH	α-FeOOH	Co_3O_4, $Co(OH)_2$			α-$Co(OH)_2$	CoOOH	α-$Co(OH)_2$	α-$Co(OH)_2$	
shape	polyhedral, rodlike	spherical	cubic	irregular			irregular	cubic	irregular	irregular	
mean size $\pm$ SD, nm	19 ± 5, $(94 \pm 24) \times (17 \pm 2)$	12 ± 3	17 ± 7	20 ± 4	>200 poly-dispersed		>300 poly-dispersed	90 ± 24	>300 poly-dispersed	>300 poly-dispersed	
superparamagnetic	yes	non	non	yes	yes	non	yes	yes	yes	yes	non

chloride salt. Linear aggregates were scarce in this sample. The average particle size was similar to that in composites from sulfate salt but the size distribution was narrower (Table 2).

PMH−Mn(II) materials were apparently free of particles. However, all the materials prepared from cobalt salts by the heterogeneous method contained crystalline nanoparticles. Examples of the texture of PMH−Co(II) composites as observed by TEM are presented in Figure 4. Particles found in polyimine cobalt composites are mainly $Co(OH)_2$. Their average size is larger than that in iron composites obtained by a similar procedure. They also show a better-defined shape and are rarely agglomerated.

Influence of the Anion Ligand. The type of anion ligand in the precursor salt does not affect the rate of reaction. However, it influences the size, shape, and crystalline phase of the precipitated nanoparticles. It can be appreciated in Table 2 that sulfate ions promote the formation of the oxide phase (Co_3O_4 in the case of cobalt and α-Fe_2O_3 in the case of iron), and chloride ions produce particles with a larger average size and a narrower size distribution.

Influence of the Solvent. The effect of the solvent was also studied. With respect to pure water, the complex formation reaction is accelerated in ethanol, in methanol, and especially in water−acetone mixtures. The polymer/metal ratio also varies with the solvent. The amount of cobalt ions coordinated in a PMH matrix increases substantially when the reaction is carried out in ethylene glycol or glycerin (Table 2). Moreover, the solvent is affecting the crystalline phase and the size of precipitated particles. The occurrence of the CoOOH phase increases with respect to the $Co(OH)_2$ phase, and the particle size and size dispersion decreases, when switching from water to ethanol. Therefore, ethanol is apparently enhancing the hydrolysis of metal ions.

Influence of Additives. Several materials were prepared under special conditions to investigate the process of formation of the nanoparticles. The formation of iron oxide particles always involves oxidation of iron(II) to iron(III). Thus, samples of PMH−Fe were prepared from chloride salts in the presence of EDTA, an Fe(III) complexing agent. The result was not an absence of particles but a broadening of the particle size distribution (SD = 41%) and a rounding of the particle shape. Then, some PMH−iron(II) samples were prepared from chloride salts in the presence of an antioxidant agent such as dithionate. The resulting materials also contained particles, in this case with a narrower size distribution (SD = 24%).

Influence of the Preparation Method. Some samples were produced by the homogeneous method of mixing a solution of PMH in chloroform and a solution of $CoSO_4$ in water. These samples were free of particles.

Magnetic Properties of PMH−Metal Complex Materials. Figure 5 shows the temperature dependence of the in-phase component of the magnetic susceptibility, χ', for iron and cobalt polymer−metal samples. The $\chi'(T)$ curve corresponding to the PMH−Co complex material shows a maximum at 11 K and then decreases monotonically. Figure 6 shows that the temperature of the susceptibility maximum increases with the frequency of the alternating field. This is a typical super-

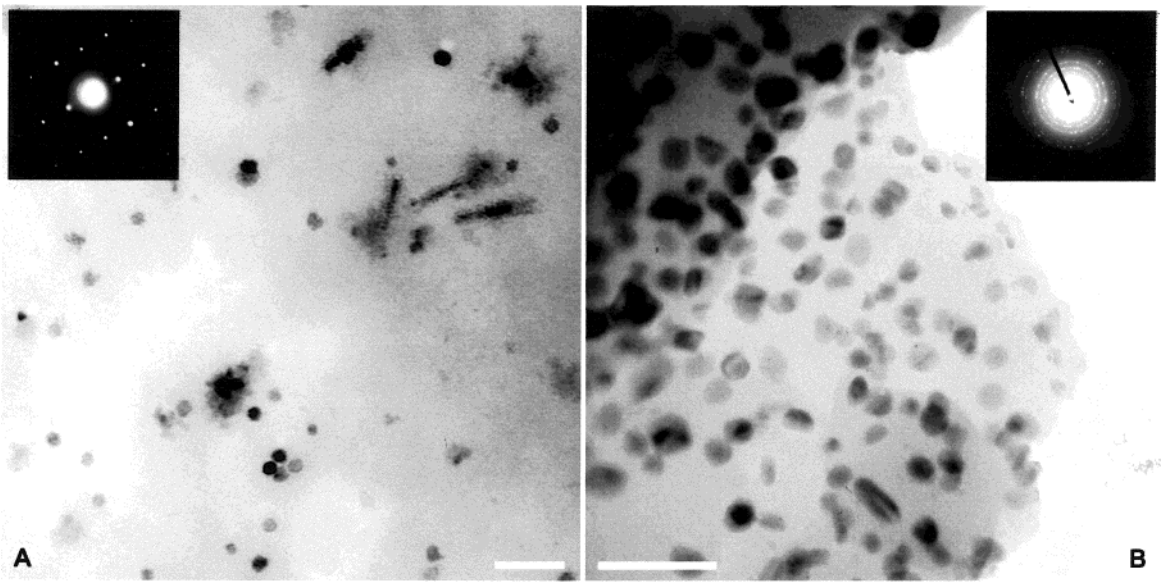

Figure 3. EM micrographs and electron diffraction patterns of PMH−Fe samples obtained from, A, $FeSO_4 \cdot 7H_2O$ and B, $FeCl_2 \cdot 4H_2O$. The length of the white bar at the bottom corresponds to 100 nm in both pictures.

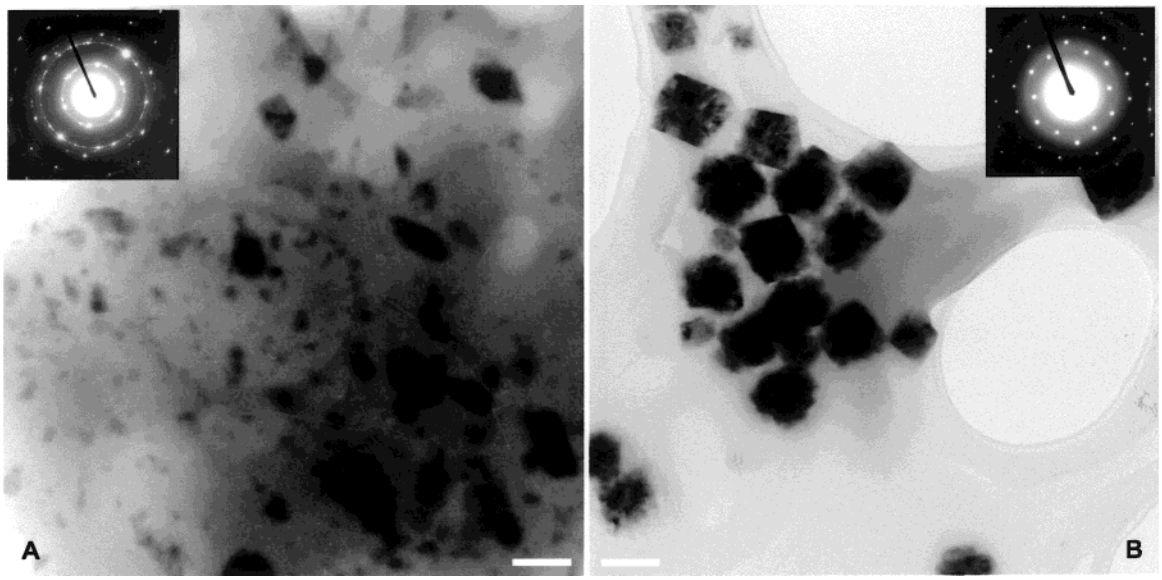

Figure 4. EM micrographs and electron diffraction patterns of PMH−Co samples obtained from, A, $CoSO_4 \cdot 7H_2O$ and, B, $CoCl_2 \cdot 6H_2O$. The length of the white bar at the bottom corresponds to 100 nm in both pictures.

paramagnetic behavior.[38] The $\chi'(T)$ curve for PMH−Fe is apparently that of a paramagnet. However, subtracting the paramagnetic contribution to the curve yields the typical $\chi'(T)$ curve of a superparamagnet with a blocking temperature $T_B = 50$ K. Thus, the magnetic properties of this sample can be explained as a summation of a paramagnetic behavior related to Fe(II) ions coordinated to the imine groups and a superparamagnetic contribution due to the nanoparticles of Fe(III) oxides observed in the EM examination of the sample. Figure 7 shows a comparison of the temperature dependence of χ' for PMH−Co materials prepared from different Co(II) salts. It can be appreciated that blocking temperature (T_B), susceptibility maximum (χ'_{max}), and even the shape of the $\chi'(T)$ curve vary significantly among the several materials.

PAH−Metal Complex Materials. In another set of experiments, polymer−metal materials were prepared from PAH. Estimations by NMR yield a polymer chain length of 10 units. The terminal groups in the polymer chain are amine groups. The capability of these groups to coordinate metallic ions is considerably less than that of tridentate imine ligands. Thus, we do not expect any important participation of the amine groups in the reaction of the polymer with the metal solution or in the precipitation of the particles inside the polymer matrix. We did not observe any appreciable end effect by IR. As was observed for PMH, the reaction of PAH with an iron salt or a cobalt salt involves a shift of the IR imine band and an increase in thermal stability (Table 1). Figure 8 shows the large change in the X-rays diffraction spectrum experimented by PAH powders after reaction with an $FeSO_4$ solution. The results of optical microscope observations of the reaction on PMH

(38) Palacio, F. In *Localized and itinerant Molecular Magnetism. From Molecular Assemblies to the Devices*; Coronado, E., Delhaes, P., Gatteschi D., Miller, J. S., Eds.; Kluwer Academic Publishers: Amsterdam, 1996.

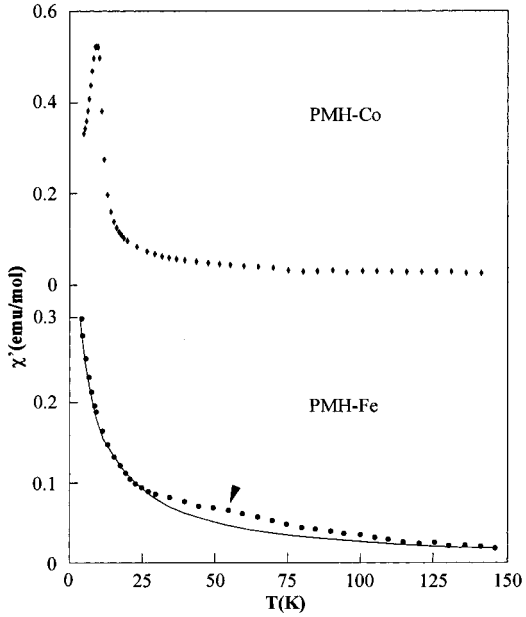

Figure 5. Variation of the ac magnetic susceptibility χ' with the temperature for PMH−Fe and PMH−Co samples obtained from chloride salts. The solid line corresponds to the fitting to a Curie−Weiss relation. The arrow indicates the point of maximum deviation from the Curie−Weiss relation.

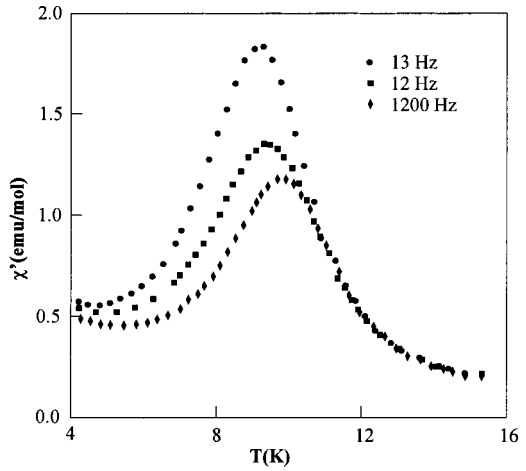

Figure 6. Variation of the ac magnetic susceptibility χ' with the temperature for a PAH−Co sample, for several frequencies of alternating magnetic field.

can also be extended to PAH, except for the longer reaction times observed in the later. In fact, PAH−Co complex materials had to be prepared in methanol because the reaction in water was too slow. Data about the preparation, composition, and magnetic properties of the samples are given in Table 3. The $\chi'(T)$ curves for PAH−Co samples prepared from hydrated salts show the typical maximum of superparamagnets (Figure 9). However, The $\chi'(T)$ curves for PAH−Co materials from anhydrous chloride salt fit well to a Curie−Weiss relation. PAH−Fe samples from chloride and sulfate salts are also paramagnetic. We examine some of the PAH−metal materials by TEM. As expected, PAH−iron samples did not contain crystalline particles. PAH−cobalt samples prepared from perchlorate salts contained particles that consisted of CoO according to electron diffraction measurements. The contour of the particles was not clear from the EM images as they were

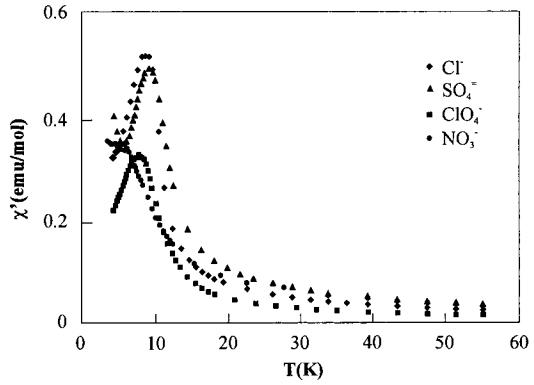

Figure 7. Variation of the ac magnetic susceptibility χ' with the temperature for several PMH−Co samples obtained from different cobalt salts.

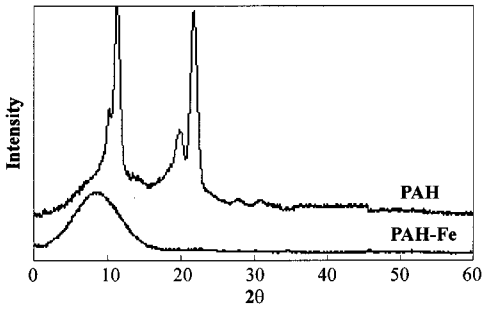

Figure 8. X-ray diffraction patterns of PAH and the PAH−Fe complex obtained from $FeSO_4$.

often overlapping. Therefore, it was not possible to perform a particle size analysis of the sample, although it was apparent that the size distribution was quite broad. Samples of PAH−cobalt prepared from chloride salts also contained particles. These had a polyhedral shape and a size between 50 and 100 nm. The elemental microanalysis of particles with EDS showed a high concentration of chlorine in the particles. Their electron diffraction patterns showed spots that could be assigned to the monoclinic structure of $CoCl_2 \cdot 6H_2O$, together with some weaker spots that corresponded with the CoO cubic structure.

Discussion

One could expect that the reaction of the polymer powders with the metal solution proceeds by diffusion of the metal ions into the polymer grains. However, optical microscopy observations show that the reaction begins at surface imperfections and it is hindered on flat surfaces. Moreover, the polymer and the polymer−metal complex material have a very different texture and they are loosely attached to each other. Furthermore, X-ray powder diffraction patterns indicate extensive structural changes during the formation of the polymer complex material. Therefore, the reaction is likely to occur by a surface process. This process can take place in three steps: complexation of surface polymer chains, separation of the complex chains from the polymer solid phase, and rearrangement of the polymer complex chains to form a different solid phase. In this way, the reaction involves both a solvation of surface polymer chains, which have apolar parts and polar moieties, and a solvation of inorganic ions, essentially polar. Consequently, the reaction is enhanced

Table 3. Preparation and Magnetic Properties of PAH Composites

	salt						
	$FeSO_4 \cdot 7H_2O$	$FeCl_2 \cdot 4H_2O$	$CoSO_4 \cdot 7H_2O$	$CoCl_2 \cdot 6H_2O$	$CoCl_2$	$Co(NO_3)_2 \cdot 6H_2O$	$Co(ClO_4)_2 \cdot 6H_2O$
solvent	water	water	methanol	methanol	methanol	methanol	methanol
method	standard	standard	standard	standard	completely anhydrous	standard	standard
[monomer]/[metal]	2	1	2	2	2.2	2	2
superparamagnetic	non	non	yes	yes	non	yes	yes

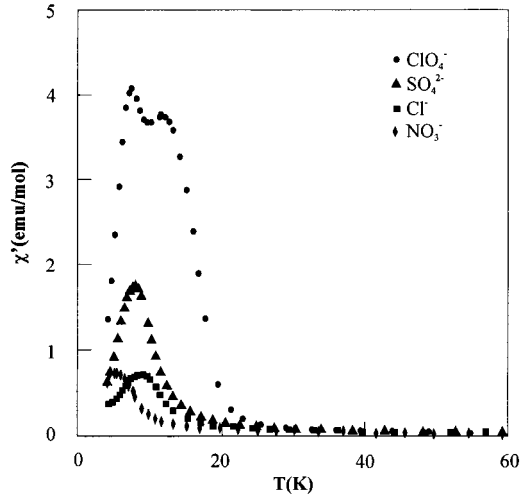

Figure 9. Variation of the ac magnetic susceptibility χ' with the temperature for several PAH−Co samples obtained from different cobalt salts.

in mixtures of water and organic solvent, and it runs faster for PMH than for PAH, which has an extra hydrophobic radical (methyl) on the imine groups.

We may have some insight onto the structure of the polymer−metal material. Studies by EXAFS revealed the presence of metal−polymer complexes, in which the metal ions are octahedrally coordinated to two tridentate planar residues situated in perpendicular planes.[35] It is feasible for two consecutive residues in a chain to link to the same metal ion, but this pattern is unlikely to repeat along the whole chain.[31] Thus, a part of the metal ions will be shared by neighboring chains, building a cross-linked structure as proposed for other Fe(II)−polymer complexes.[20] That explains the low solubility and the high melting point of polymer−metal materials. The complex polymer chains are expected to stack, matching their polar and apolar groups among themselves in order to minimize the packing energy. That would create polar regions inside the polymer matrix that can be filled by solvated ions. In fact, we have observed that polystyrene, which does not form any complex with Co(II) ions, can incorporate a 3% weight of $CoCl_2$ salt. These metal−water solvates trapped in polar nanoregions would hydrolyze easier than the metal ions coordinated to the imine groups. Thus, it is likely that they are the origin of the metal oxide nanoparticles appearing in the polymer matrix. The fact that only those PMH−metal materials prepared in anhydrous conditions were free of particles supports this mechanism.

The hydrolysis of metal ions in polyimine matrixes occurs readily without addition of a base because the imine groups provide a local basic media. Consequently, PMH is more efficient than PAH for the production of metal oxide particles because it is more basic. The formation of Fe(III) oxides from Fe(II) salt precursors is not surprising because the Fe(II) ions are easily oxidized to Fe(III). The addition of Fe(III) complexing agents or antioxidants to the reaction medium does not stop this process. However, these experiments reveal that additives can modify the average size and the size distribution of the particle population.

To understand the process of particle formation within the polymer matrix, it is worthy to compare it with the well-known process of hydrolysis of metal ions in solutions.[39,40] The first step in the hydrolysis of Fe(III) ions in aqueous solutions is the formation of soluble iron polymers. These polymers are converted into gels composed of polycations in a fractal arrangement. The hydrolysis continues with the precipitation of amorphous iron oxohydroxides that later transform into hematite (α-Fe_2O_3) or goethite (α-FeOOH). One of the advantages of polyimine polymer matrixes is that the amine compounds accelerate the hydrolysis of iron(III) ions.[41] It has been often reported that the type of counterion in the precursor metal salt largely affects the hydrolysis of metal ions. That explains the differences of texture and magnetic properties that we found among nanocomposites prepared from different metal salts. In the solution process, when the counterion restrains the transformation of amorphous ferrihydrite into a crystalline phase, the most stable phase, hematite, is formed. This effect increases in the order nitrate < chloride < sulfate.[42] Therefore, the oxide phase is frequent in our nanocomposites prepared from metal sulfate salts. It is also known in solution hydrolysis that Cl^- ion ligands get into the coordination sphere of the metal ions and they are difficult to replace by OH^- ions.[39,43] Then, crystal growth and particle aggregation is restrained.[43] That can be the reason the particle size distribution in nanocomposites from chloride salts is narrow. The different crystal shapes that we found in nanocomposites from different metal salts can also be explained by an effect of the counterion. It is known that sulfate ions have a large affinity for iron oxide crystal surfaces that favors a rounded shape while chloride ions are preferentially adsorbed on specific planes inducing a prismatic habit.[43] The distribution, size, and number of particles are also governed by the kinetics of the drying process, the solvent, and the presence of foreign substances. It has been found that nanoparticles in PMH−Co composites prepared in ethanol have a lower particle size dispersion than those prepared in water. This can be explained because $Co(H_2O)_6^{2+}$ solvates will

(39) Tchoubar, D.; Bottero, J.-Y. *C. R. Acad. Sci. Paris IIa* **1996**, *322*, 523.
(40) Flynn, C. M., Jr. *Chem. Rev.* **1984**, *84*, 31.
(41) Kandori, K.; Yasukawa, A.; Ishikawa, T. *J. Colloid Interface Sci.* **1996**, *180*, 446.
(42) Parida, K. M.; Das, J. *J. Mater. Sci.* **1996**, *31*, 2199.
(43) Park, G. S.; Shindo, D.; Waseda, Y.; Sugimoto, T. *J. Colloid Interface Sci.* **1996**, *177*, 198.

have a larger tendency to associate in an aqueous medium than in ethanol and that will result in irregular growth.

Conclusion

Magnetic nanocomposites can be prepared from imine polymers by a very simple procedure. The reaction of the polymer with a metal solution yields a polymer−metal complex material, which generates nanoparticles after drying at moderate temperature without any treatment with a base or an oxidizing agent. The complex formation reaction can be explained as a surface reaction process involving polymer chain reorganization. In accordance with this mechanism, the rate of reaction is enhanced by mixtures of water and organic solvents. The production of nanoparticles works the best for polymers with a flexible chain that do not contain hydrophobic branches and for Co(II) ions as compared to Fe(II) ions. The particles are probably formed from metal solvates encapsulated within polar nanoregions of the polymer complex material rather than from coordinated metal ions. The characteristics of the nanocomposite are greatly influenced by the type of anion ligand in the precursor metal salt.

Acknowledgment. We are indebted to J. Garín, J. Reyes, and J. Fernández for their assistance and helpful discussions. Financial support from CICYT (MAT97-951) is gratefully acknowledged.

CM0011561